

Calibration of an Existing Creep Model for Analysis of Aluminium Members Exposed to Constant Temperature

Marko Goreta, Neno Torić, Ivica Boko

University of Split, Faculty of Civil Engineering, Architecture and Geodesy, Matice hrvatske 15, 21000 Split, CROATIA
e-mails: marko.goreta@gradst.hr; neno.toric@gradst.hr, ivica.boko@gradst.hr

SUMMARY

The paper presents the development of a creep model applicable for the analysis of aluminium members exposed to a constant temperature. The model is intended as a base for defining a creep model in a transient heating regime. The behaviour of aluminium members exposed to the transient heating regime is a relatively unexplored topic in the scientific community. There is a need for defining an advanced creep model for aluminium, which should cover any heating regime to model the influence of creep on members exposed to fire. A comparison of results between the existing experimental data and the built-in creep models from commercial software ANSYS 16.2 for specific temperature and stress levels is provided. The experimental data used was extracted from previous tests carried out on coupons of aluminium alloy EN 6082 AW T6 and fitted in the aforementioned ANSYS models which serve as a base for defining the representative advanced creep model.

KEY WORDS: aluminium; creep; fire; column; coupon; tests; EN 6082 AW T6; ANSYS 16.2.

1. INTRODUCTION

1.1 ALUMINIUM IN CIVIL ENGINEERING

Aluminium is currently considered a building material of the future because of its favourable mechanical properties compared to standard construction steel. Notable worldwide quantities also favour more frequent use of aluminium alloys in everyday construction.

A significant number of structures worldwide are made of aluminium [1]. Some examples include a road bridge Arvida over the river Saguenay in Quebec, Canada and pedestrian bridge Hem-Lenglet in Hauts-de-France. The former is entirely made of aluminium, weighs around 200 tons with a total span of 153.62 meters, and an arch span of 91.5 meters while the latter is of a total length of 83 meters and the main-span length of 63 meters. Besides the aforementioned bridges, aluminium is used for building antenna towers in Italy, Naples,

lightweight roof constructions, industrial objects (domes for coal storage in China, Caofeidian), facades, pipelines, tanks, etc.

1.2 COMPARISON OF ALUMINIUM WITH STEEL

Mechanical properties of aluminium at room temperature compete very well with standard construction steel (Table 1.). For example, aluminium alloy EN 6082 AW T6 used in this study has a minimum proof strength above 260 MPa at room temperature which is equivalent to the yield strength of steel S275, mainly used in everyday structures in Europe.

Table 1 Comparison between the basic properties of aluminium alloys and steel

<i>Physical properties / Metal</i>	<i>Aluminium / Al alloys</i>	<i>Steel</i>
<i>Melting point</i>	660 °C	1425 – 1540 °C
<i>Density at 20°C</i>	2700 kg/m ³	7850 kg/m ³
<i>Linear thermal coefficient</i>	23 · 10 ⁻⁶ °C ⁻¹	12 · 10 ⁻⁶ °C ⁻¹
<i>Modulus of elasticity</i>	70 000 N/mm ²	210 000 N/mm ²
<i>Shear modulus</i>	27 000 N/mm ²	81 000 N/mm ²
<i>Poisson's ratio</i>	0,3	0,3

The primary advantages of aluminium over steel are:

- Corrosion resistance – significant savings in anti-corrosion agent and building maintenance,
- Low density – greatly simplifies construction process due to reduced structural weight compared to steel (around 2.9 times lighter),
- Simple design and extrusion of structural elements – material savings due to better structural usability (no sparking in processing).

Other essential features include very good light and heat reflection. Aluminium is neither ferromagnetic nor toxic, and it has no negative impacts on the environment.

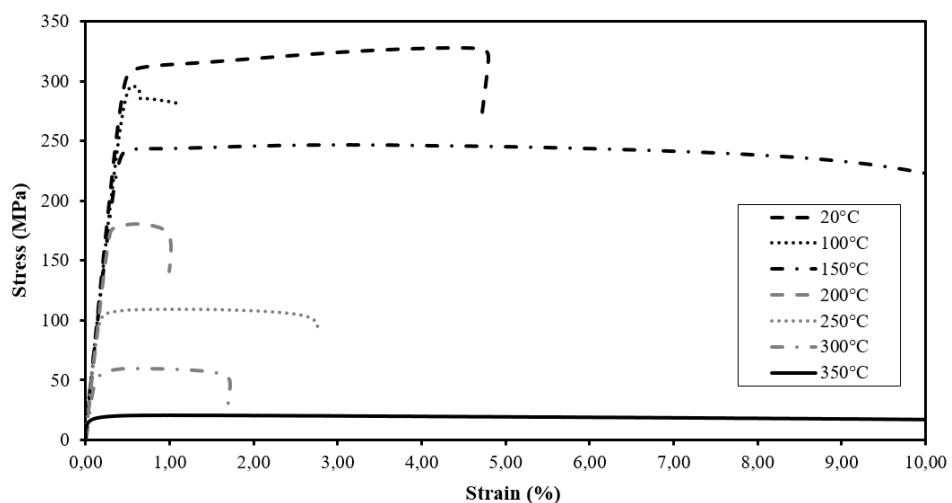


Fig. 1 Stress-strain curves at high-temperature for aluminium alloy EN 6082 AW T6 [2]

Besides the mentioned advantages, aluminium has some disadvantages like relatively high cost and vulnerability to high temperature because of a significant decrease of load-bearing capacity starting from 150-200°C presented in Figure 1. The hypothesis for the unreasonable ductility intervals is related to the material properties of aluminium having variable temperature-dependent ductility.

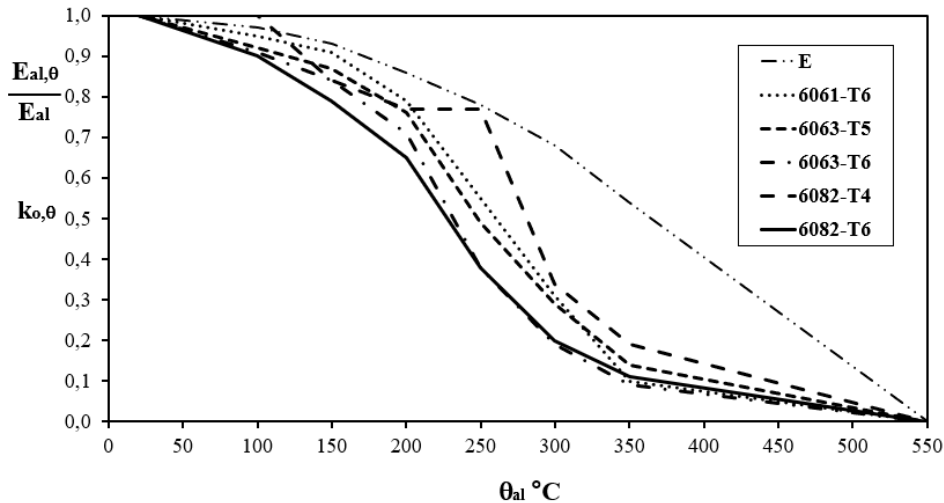


Fig. 2 Ratio of conventional yield point for 0.2% proof strength $k_{0,\theta}$ and $E = E_{al,\theta}/E_{al}$ for EN 3004 AW H34 and EN 6xxx aluminium alloys on elevated temperature $\theta_{al}/^{\circ}\text{C}$ for two hours thermal exposure [3]

Figure 2 presents a decrease of the modulus of elasticity, E , on high temperatures for different aluminium alloys of 6xxx series for two hours thermal exposure and its reflection on its yield strength. It is shown how the difference in tempering (treating of aluminium in its production process) between $T4$ and $T6$ for alloy 6082 causes notable differences on E and $k_{0,\theta}$. The assumption is that the irregular curves are related to the material characteristics of the aluminium microstructure, similar to the ductility problem explained above.

The behaviour of aluminium structures exposed to fire, especially concerning the transient heating regime, represents a relatively unexplored scientific topic. This topic is only partially covered by present design codes [3]. The impact level of creep on the load-bearing capacity of aluminium beams and columns exposed to high temperatures is valuable due to the consideration of possible structural failure mechanisms. The conclusions based on studies [4-10] point out that creep has a significant influence on the reduction of the collapse time of the structure when certain thermo-mechanical conditions are present.

2. CREEP

2.1 GENERAL

As is known, creep is a time-dependent inelastic deformation that occurs over time when a constant load is applied at a high temperature. It is significantly influenced by the material chemical composition and crystal structure. It is an irreversible process in which the long molecular chains slide along each other, with the effect of reducing the overall load-bearing capacity of the structural member. For aluminium, the significant creep strain occurs at a

temperature over 160°C [2], and its impact depends on the magnitude of the applied load. The main assumption is that the higher load and temperature accelerates the failure process due to creep.

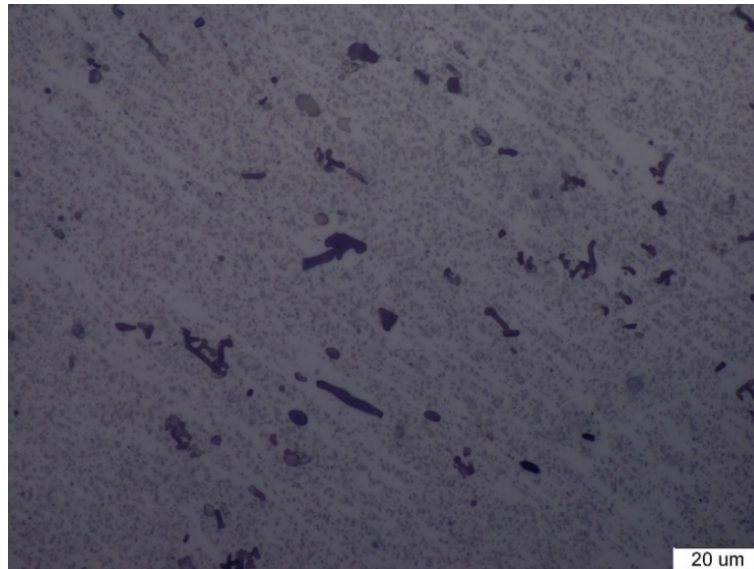


Fig. 3 EN 6082 AW T6 microstructure with 1000x magnification at room temperature

Figure 3 presents the microstructure of aluminium which consists mainly of pure aluminium particles and large chemical compounds with other alloying elements. The chemical composition of EN 6082 AW T6 alloy is shown in Table 2. A higher load level and heating regime increase molecular cavities. It accelerates the process of the development of the creep strain and thus affects the structural analysis shortening the time of structural failure.

Table 2 Chemical composition of aluminium alloy EN 6082 AW T6 [2]

<i>Symbol</i>	<i>Al</i>	<i>Cu</i>	<i>Si</i>	<i>Fe</i>	<i>Mn</i>	<i>Mg</i>	<i>Zn₂</i>	<i>Cr</i>	<i>Ca</i>	<i>Pb</i>	<i>Rest</i>
%	96,49	0,099	1,281	0,708	0,523	0,767	0,0615	0,0141	0,0011	0,0034	0,0519

2.1.1 STATIONARY CREEP DEVELOPMENT

Development of creep strain at constant (stationary) temperature regime is well known and can be divided into three phases (Figure 4):

- Primary phase- creep strain consisting of an elastic and plastic part. Creep strain occurs rapidly and then it slows in time, which is due to strain hardening of the material (including elastic strain ϵ_0 at time index t_0);
- Secondary phase- stable creep strain development (constant strain rate);
- Tertiary phase- a sudden increase in strain caused by the impairment of the material microstructure which leads to fracture.

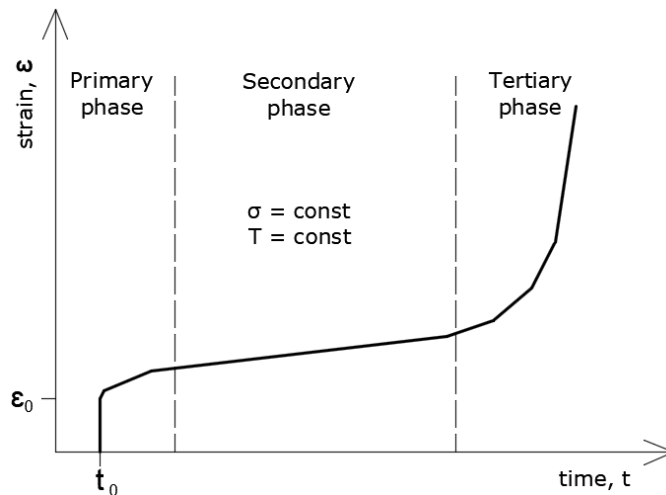


Fig. 4 Stationary creep phases

2.1.2 TRANSIENT CREEP DEVELOPMENT

The development of creep concerning transient heating is different in terms of the shape of the creep strain curve. The primary indicator for the transient-creep rate is the heating rate value expressed as the $\dot{T} = dT/dt$ ratio. Given that, the main goal is to achieve the constant heating rate during the experiments by selecting an appropriate heating regime. The transient creep model is used to analyse the behaviour of fire exposed members more realistically (since fire action is transient in nature). Generally, lower heating rates (range $1-10^{\circ}\text{C}/\text{min}$) correspond to the possible heating rates induced in members when fire protection is applied (insulation, coatings, or sprayed protection).

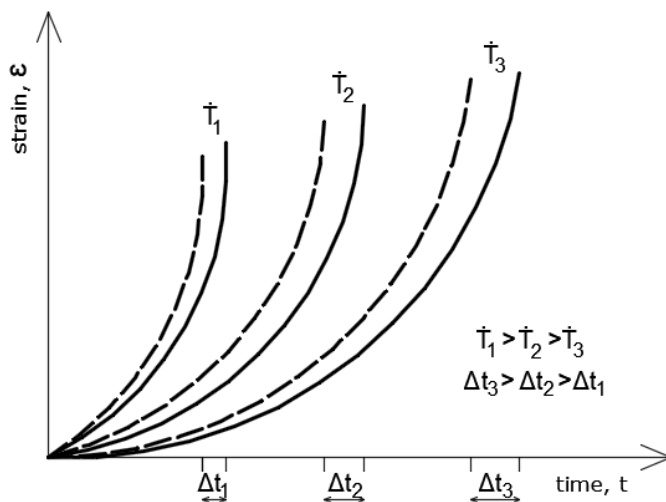


Fig. 5 Comparison between the creep-free response and the creep-included response of aluminium

The influence of various heating rates (\dot{T}) in the transient analysis is presented in Figure 5, where the full-line curves represent a creep-free response and the dashed curves take into account the influence of creep in terms of the time-strain ratio. The main objective of the ongoing research topic is to investigate the level of reduction of failure time of columns due to creep initiated by transient heating.

2.2 OVERVIEW OF CREEP MODELS

Hardening is a process where metal hardens after passing its yield point and increases its resistance to plastic deformations. When analysing the creep response of aluminium exposed to high temperature, there are two types of available creep models based on strain-hardening or time-hardening rules.

The strain-hardening applies for thermo-mechanical conditions where the stress level changes significantly over time during fire exposure. According to Harmathy [5], this makes the creep strain rate a function of stress and the previously accumulated creep strain.

The time-hardening presented by Harmathy [11] is related to thermo-mechanical conditions where stress level changes negligibly over time, assuming that the creep depends exclusively on time and stress level.

The creep solutions for the described thermo-mechanical conditions can be obtained through analytical, semi-empirical, and rheological models.

The base for analytical research of creep in metals was proposed by Dorn [4] and Harmathy [11], as a function of stress and temperature-compensated time provided by the following equation:

$$\varepsilon_t = \varepsilon_t(\theta, \sigma) \text{ for } \frac{d\sigma}{dt} = 0 \text{ when } t > 0 \quad (1)$$

Where the temperature θ is defined as:

$$\theta = \int_0^t e^{-\Delta H/RT} dt \quad (2)$$

ΔH is the increment for the Zener-Hollomon parameter (h^{-1}), R universal gas constant ($J/mol^\circ K$), and T is the temperature ($^\circ K$).

By differentiating Eq. (1), the expression for the creep rate is obtained:

$$\frac{d\varepsilon_t}{dt} = \frac{\partial \varepsilon_t}{\partial \theta} e^{-\Delta H/RT} \quad \left(\frac{d\sigma}{dt} = 0 \right) \quad (3)$$

Described creep model proposed by Dorn was validated in transient heating conditions by numerical analysis of Harmathy [5], based on the lattice model, and compared with three fire protection tests. The numerical procedure covered the subdivision of the member into sections while the temperature was measured in three points: lower flange, upper flange, and at the centre of the web with the unknown heating rates. Comparison of the experimental and numerical results showed a very good match for all three tests.

More recent semi-empirical studies were carried out by Maljaars [7-9], based on the aforementioned theory given by Dorn and Harmathy. Maljaars adapted an existing model (1) for fire-exposed aluminium alloys in transient state tests and modified it to be suited for 6xxx alloys.

Simulation of transient state tests was expressed with Eq. (4):

$$\varepsilon = \frac{\sigma}{E} + \int_0^t \dot{\varepsilon}_{t,I+II} dt \quad (4)$$

where the creep strain at the end of each time-step i is obtained based on the creep strain in the previous time-step $i-1$, creep strain increment, activation energy Q (J/mol), and Zener-Holloman parameter Z (h^{-1}).

$$\varepsilon_{t,I+II}^i \approx \varepsilon_{t,I+II}^{i-1} + Ze^{-Q/RT} \coth\left(\frac{\varepsilon_{t,I+II}^{i-1}}{\varepsilon_{t0}}\right) \Delta t \quad (5)$$

Based on Eq. (5), Maljaars modified the constitutive model to successfully cover the primary, secondary, and the first part of tertiary creep phases:

$$\dot{\varepsilon}_{t,III} = C \dot{\varepsilon}_{t,I+II+III} \quad (6)$$

where C is elaborated with the creep strain-rate start of the tertiary stage ε_{lim} .

$$C = \frac{\dot{\varepsilon}_{t,I+II}}{\varepsilon_{lim}} \quad (7)$$

The rheological models used for creep modelling are defined as a combination of two types of elements: the spring element, which represents the general non-linear stress-strain relationship, and the Kelvin-Voight element, used for the development of stress-related strain and creep strain component. The general concept of the rheological model is presented by Helman and Creus [12] for the non-linear time-dependent strain in the case of constant stress at room temperature. Torić et. al [13] adapted the aforementioned model to represent the creep behaviour of steel and aluminium at constant high-temperature. Furthermore, Torić and Burgess [14] developed a unified rheological model for the analysis of strain development in steel at high-temperature in the case of transient heating.

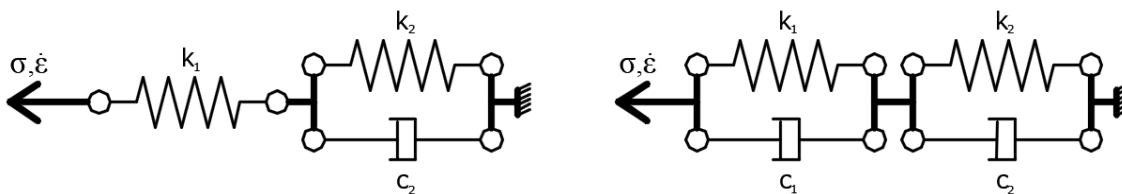


Fig. 6 Rheological models a) R1 (left) b) R2 (right)

The R1 rheological model presented in Figure 6.a can be used in case of moderate strain rates. It comprises a spring element representing the stress-related strain component, and the Kelvin-Voight element representing the creep strain component. The stress-strain relationship (σ), for the spring element, can be expressed with the equation:

$$\sigma = k_1(\sigma, T) \varepsilon_1 \quad (8)$$

While the differential equation for the Kelvin element expressed with k_2 and c_2 is:

$$\frac{\sigma}{c_2(\dot{\varepsilon}, T)} = \frac{k_2(\sigma, T)}{c_2(\dot{\varepsilon}, T)} \varepsilon_2 + \dot{\varepsilon}_2 \quad (9)$$

For total strain rate ($\dot{\varepsilon}$) to be computed as:

$$\dot{\varepsilon} = const = \dot{\varepsilon}_1 + \dot{\varepsilon}_2 \quad (10)$$

with $\dot{\varepsilon}_1$ strain rate for the spring element, and $\dot{\varepsilon}_2$ for the Kelvin-Voight element.

R2 rheological model presented in Figure 6.b is used in case of lower strain rates, and it is a combination of two Kelvin-Voight elements where the first one represents the stress-related strain component which takes into account the apparent increase of yield strength due to inertia effect, and the second represents creep strain component.

The differential equation for each of the Kelvin elements in the R2 model can be expressed as:

$$\frac{\sigma}{c_i} = \frac{k_i}{c_i} \varepsilon_i + \dot{\varepsilon}_i \quad (11)$$

For $i = 1, 2$. The total strain rate ($\dot{\varepsilon}$) can be expressed as the total strain on the Kelvin element for the R1 model (10). The problem of two differential equations can be solved by the Euler integration using the smaller time increments.

The c_1 and c_2 presented in the equations above are damping coefficients with experimentally determined temperature and strain-rate dependency, and the k_1 and k_2 are the spring models which represent the experimentally determined stress-related strain.

3. FORMULATION FOR THE STATIONARY CREEP MODEL AND THE VALIDATION OF THE RESULTS

3.1 CREEP MODELS AND EQUATIONS

Experimental results for the creep strain development were obtained as a function of time, temperature and stress from the previous study of aluminium alloy EN6082AW T6 by Torić et al. [2]. The tests were performed on coupons at three different stress levels (generally on stress levels of 0.2, 0.3, 0.5, and 0.7 of σ_{max} , which represents stress just before failure from capacity tests loaded axially for temperatures of 150, 200, 250, and 300°C) with a visible representation of the transition between the creep stages. The capacity tests were conducted based on the ASTM standards [15,16] for every given temperature with a load of 10 MPa/s. The analytical creep law [2] was proposed for specified temperatures and stress levels.

The main objective of the planned research campaign is to develop a suitable creep model for aluminium alloy EN6082AW T6 capable of taking into account the development of creep in a transient heating regime. The developed creep model at constant temperature represents a base for analysis of the transient heating tests on aluminium columns that require further research. Considered that, and in order to model the creep behaviour of aluminium at high-temperature precisely, it is necessary to define a creep model for stationary heating conditions that is valid for all temperature levels and their corresponding stress levels. With that aim, the commercial software ANSYS Workbench 16.2 [17] was selected to validate the available experimental data since it has a rich library of creep models.

Software ANSYS offers thirteen different creep models with user-defined options available. For this study, only two creep models are considered for comparison due to simplicity and the validation of the different creep phases. The first model covers only the primary phase and utilizes the time-hardening method with continuous tracking of stress change due to its main impact on creep strain in time. The second model was chosen to observe how the creep deformation manifests in the secondary phase.

Table 3 ANSYS creep models with constitutive equations [17]

Model Designation	Creep model type	Equation	Creep phases
MTH	Modified Time Hardening	$\varepsilon_{cr} = C_1 \sigma^{C_2} t^{C_3+1} e^{-C_4/T} / (C_3 + 1)$	Primary
NT	Norton	$\dot{\varepsilon}_{cr} = C_1 \sigma^{C_2} e^{-C_3/T}$	Primary and secondary

In equations presented in Table 3, ε_{cr} represents creep deformation, σ is current stress (MPa), T current temperature ($^{\circ}C$), and t is the time (min) while C_1, \dots, C_4 are the coefficients of the corresponding creep model.

It can be noted that both creep models do not take into account the tertiary stage of creep. Tertiary creep can be considered relevant only for structures with a relatively small cross-section (such as prestressed wires). The coefficients for a temperature of $200^{\circ}C$, obtained by the “curve-fitting” method offered by software ANSYS, are listed in the table below.

Table 4 Coefficients for Modified Time Hardening and Norton creep models for $200^{\circ}C$

Stress	0.2f _{0.2,200} (38.1 MPa)		0.3f _{0.2,200} (57.1 MPa)		0.5f _{0.2,200} (95.2 MPa)	
	MTH	Norton	MTH	Norton	MTH	Norton
C1	5,62E-11	8,48E-61	8,20E-11	9,22E-59	9,60E-11	4,13E-58
C2	1	7,09	1	6,77	1	6,57
C3	-8,91E-01	0	-9,25E-01	0	-8,80E-01	0
C4	0	-	0	-	0	-

3.2 COUPON MODELLING

A numerical model was utilized for the validation of tensile coupon tests [2], which will be used for modelling planned transient column tests. The finite element (FE) type used in the calculation was 3D SOLID186 with quadratic displacement behaviour. Mesh was defined with FE sizing of 2 mm with medium smoothing and fast transition but without local mesh resizing. Nonlinear problem was computed with full Newton-Raphson’s method with a minimum number of substeps 1000 and maximum equilibrium iterations of 15 with automatic time stepping. Tensile testing machine jaws were simulated with one end fixed and the other sliding in a longitudinal direction, which was also the side where the load was applied.

The creep equations are integrated into ANSYS with an explicit Euler forward algorithm. A modified total strain in every substep (time step) n is computed as:

$$\{\varepsilon'_n\} = \{\varepsilon_n\} - \{\varepsilon_n^{pl}\} - \{\varepsilon_n^{th}\} - \{\varepsilon_{n-1}^{cr}\} \quad (12)$$

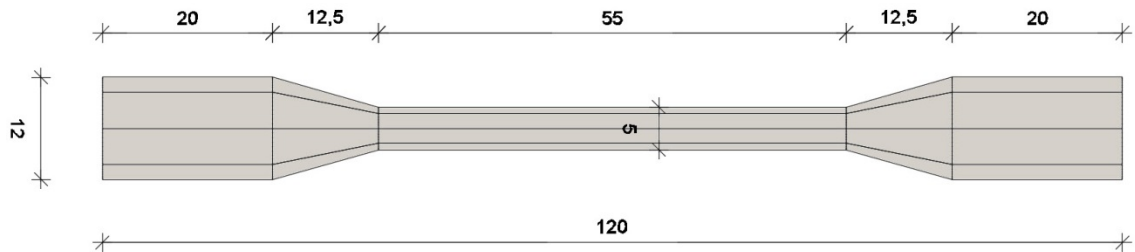
where ε is total strain vector, ε^{pl} plastic strain vector, ε^{th} thermal strain vector in current time point and ε^{cr} the creep strain vector from previous time point calculated through the equivalent creep strain increment $\Delta\varepsilon^{cr}$ for every master node m , obtained as:

$$\Delta\varepsilon_m^{cr} = \varepsilon_{et} \left(1 - \frac{1}{e^A} \right) \quad (13)$$

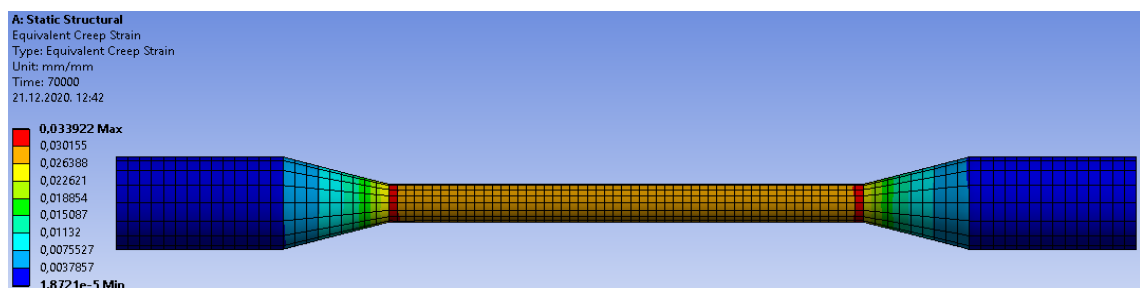
For e as the base natural logarithm, A the creep ratio, and ε_{et} the equivalent modified total strain which is expressed as:

$$\varepsilon_{et} = \frac{1}{\sqrt{2}} \left[(\varepsilon'_x - \varepsilon'_y)^2 + (\varepsilon'_y - \varepsilon'_z)^2 + (\varepsilon'_z - \varepsilon'_x)^2 + \frac{3}{2} (\gamma'_{xy})^2 + \frac{3}{2} (\gamma'_{yz})^2 + \frac{3}{2} (\gamma'_{zx})^2 \right]^{\frac{1}{2}} \quad (14)$$

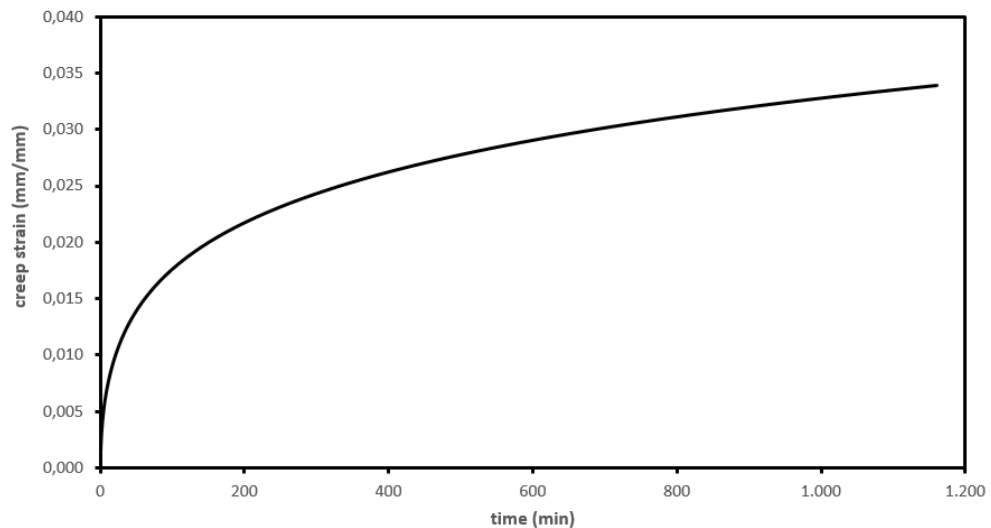
The equivalent modified total strain is calculated as a function of all three normal strain vectors ($\varepsilon'_x, \varepsilon'_y, \varepsilon'_z$) and all three shear components ($\gamma'_{xy}, \gamma'_{yz}, \gamma'_{zx}$).



a) Coupon geometry (mm)



b) FE model of the specimen with 2 mm mesh



c) Creep strain vs. time representation of the coupon at temperature of 200 °C and stress 38.1 MPa

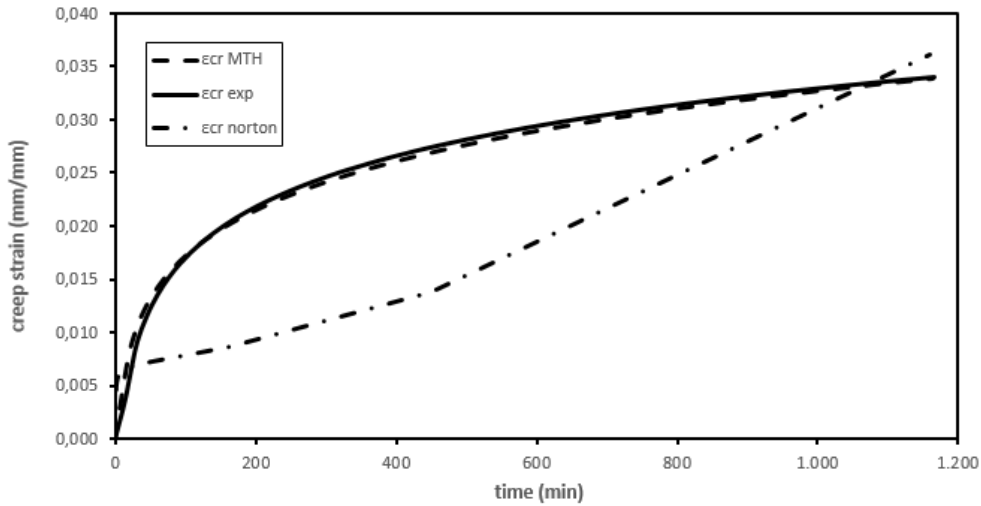
Fig. 7 ANSYS FE coupon model for aluminium alloy EN 6082 AW T6

Figure 7 presents an equivalent creep strain distribution over time for coupon tested at a temperature of 200°C and stress of 38.1 MPa, the equivalent to 0.2 $f_{0.2,200}$, which is the 20% of yield strength at 0.2% strain on 200°C for given coupon geometry. It can be seen that maximum strain is at the gauge part of the cross-section, which is the location where the coupon necking generally occurred in the tests.

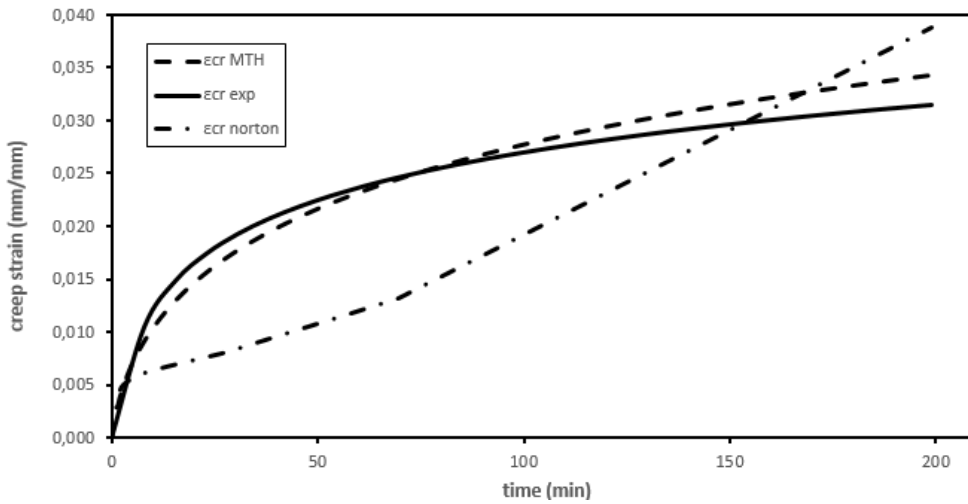
3.3 VALIDATION RESULTS

A numerical analysis of the aforementioned (Table 3) three characteristic stress values at 200°C was carried out and compared with the available experimental data [2].

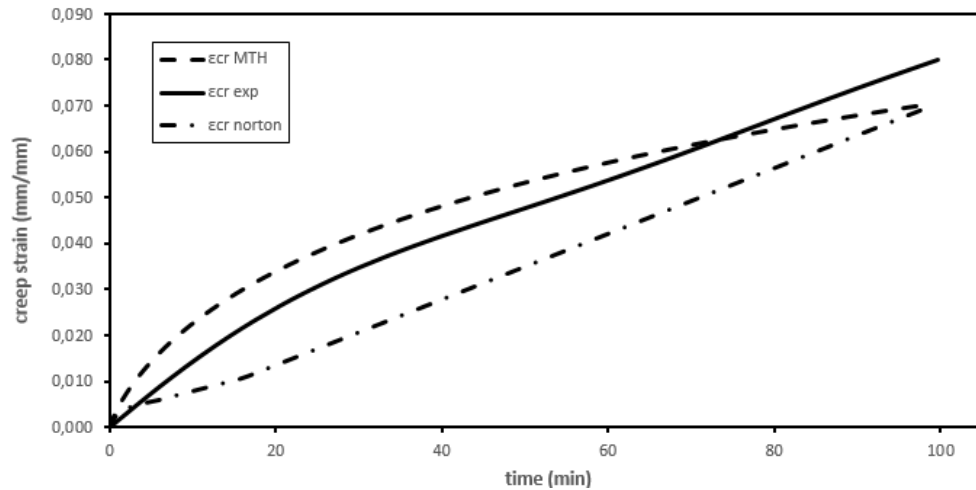
It can be observed that the Modified time hardening creep model matches very well with the experimental data [2] for all cases while the Norton creep model deviates during the experiment but ends with approximately the same value of the experimental creep strain. This is possible to occur due to different phase distribution between the two used creep models.



a) $0.2 f_{0.2,200}$ (38.1 MPa)



b) $0.3 f_{0.2,200}$ (57.1 MPa)



c) $0.5 f_{0.2,200}$ (95.2 MPa)

Fig. 8 Comparison of the results for different stress levels at 200°C of EN 6082 AW T6 coupon

It is evident from Figure 8 that the creep curves for stress levels of 0.2 , 0.3 , and $0.5 f_{0.2,200}$ have smooth-running curves for every creep model. We can observe that the creep strain for 0.2 and $0.3 f_{0.2,200}$ is nearly the same in total. However, a lower stress rate requires up to nearly five times more time to equalize the creep strain for a higher stress rate.

3.4 FEM EXAMPLE OF THE EXTRUDED I SECTION COLUMN

Numerical analysis of a dominantly axially loaded column (Figure 9) is carried out to test the validity of the Modified time hardening creep model. In addition to the axial compressive force, a transversal force is applied on the web in the middle of the column height to simulate the geometrical imperfections of the member.

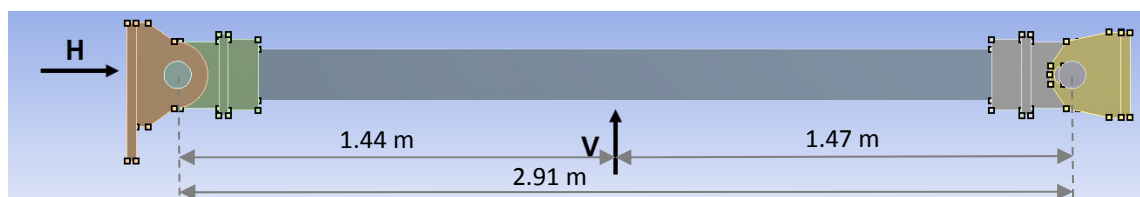


Fig. 9 Column geometry from ANSYS (side view)

The numerical model consists of two bearings, where the right was fixed, and the left used to apply the axial force on the column. The column was mounted into two pads connected to bearings with high-quality steel pins with a diameter of 50 mm made of steel S355. Same quality steel was used for pads and bearings made of several welded thick plates to achieve force transmission on the column without the occurrence of additional pad deformation, which would jeopardize the accuracy of the overall results. In the numerical model, the connection between the pads and the bearings was accomplished with the bolts. The surface of the bolts was modelled as the frictional with a standard coefficient of 0.2 suitable for two steel elements in contact.

Cross-section used for the column was I profile with a flange thickness of 14 mm and width of 170 mm . The total section height was 220 mm with a web thickness of 8 mm and the total

member length of 2579 mm. The geometry of the model used reflects an experimental setup for future transient column tests.

A numerical analysis of the column response with different loading regimes at a constant temperature of 200°C was conducted, and its creep response is illustrated in Figure 10. The loading schemes in the presented analysis are selected to demonstrate the column behaviour under the influence of stationary creep for longer time periods. It can be seen from Figure 10 that a slightly progressive increase in transverse force affects the development of the creep strain, indicating a column sensitivity to creep in case of constant temperature.

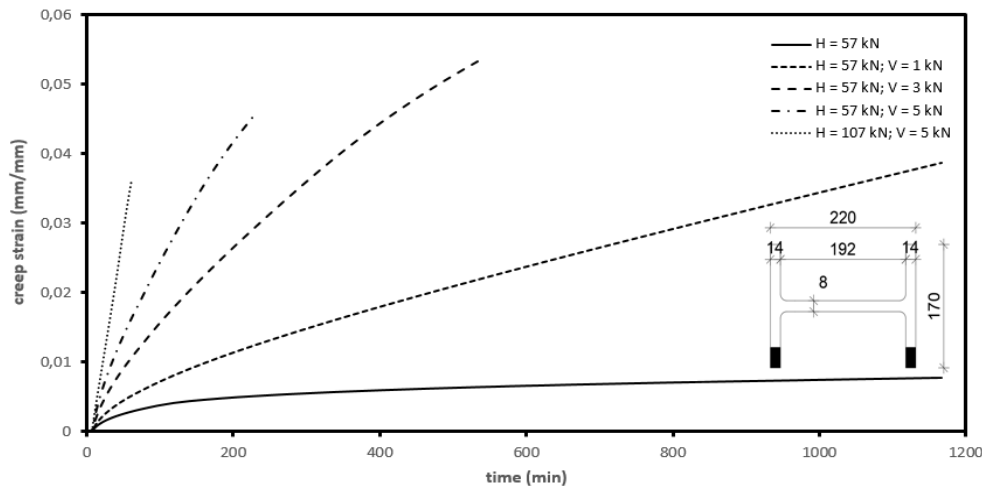


Fig. 10 Comparison of the creep strain development at different load levels for Modified time hardening model on temperature 200°C

The presented example shows that the Modified time hardening model obtained from the coupon tests and validated with a numerical example on coupons is applicable on the aluminium columns. The column response illustrated in Figure 10 shows expected behaviour due to creep and that the creep strain occurs dominantly in the compressive flange at midspan. Given results for different loading regimes support the application of this model in transient tests with different creep coefficients for multiple temperatures in a span between 160°C and 300°C.

4. CONCLUSION AND FURTHER RESEARCH

This paper presents calibration of experimental results on coupons exposed to a constant temperature of aluminium alloy EN 6082 AW T6 and fitting them into ANSYS creep models suited for stationary and transient heating conditions. Through the numerical example and shown formulations, the following conclusions are drawn:

- Adaptation of the data obtained from tests on aluminium coupons and fitting them into presented ANSYS creep models for alloy EN 6082 AW T6 at temperature 200°C for different stress levels can be performed.
- Based on the results, it can be concluded that the Modified time hardening (MTH) model matches very well with the experimental data acquired from coupon tests for specified temperature and stress levels.

- Simple numerical example on the aluminium column has shown expected results in terms of creep strain based on different loading regimes for the MTH model and coefficients acquired from coupons on the temperature of 200°C.

The proposed creep model has shown to be suitable for further analysis of the planned experimental transient tests and validation of the presented numerical model on aluminium columns. However, it is necessary to carry out a more detailed study to define unified creep model valid for transient and stationary heating conditions.

Future planned research will be oriented on transient tests in controlled laboratory conditions on EN 6082 AW T6 aluminium columns for different loading regimes in terms of the value of applied force and the heating rate.

Furthermore, coupon tests for aluminium alloy EN 6082 AW T6 are necessary for denser partitions in the temperature interval from 160°C to 300°C. The temperature span is based on recent studies [2, 18, 19] since the minimum temperature for aluminium alloy for significant creep activation is approximately 160°C. The segmentation will allow the creep strain tracking for every temperature interval with its coefficients for the specified creep model.

5. ACKNOWLEDGEMENT

This work is partially supported through project KK.01.1.1.02.0027, a project co-financed by the Croatian Government and the European Union through the European Regional Development Fund - the Competitiveness and Cohesion Operational Programme.

6. REFERENCES

- [1] D. Skejić, I. Boko, and N. Torić, Aluminium as a material for modern structures, *Gradjevinar*, Vol. 67, No. 11, pp. 1075–1085, 2015.
- [2] N. Torić, J. Brnić, I. Boko, M. Brčić, I. W. Burgess, and I. Uzelac, Experimental analysis of the behaviour of aluminium alloy EN 6082AW T6 at high temperature, *Metals* (Basel), Vol. 7, No. 4, 2017. <https://doi.org/10.3390/met7040126>
- [3] "EN 1999-1-2." Design of aluminium structures: Structural fire design, February 2007.
- [4] J.E. Dorn, Some fundamental experiments on high temperature creep, *J. Mech. Phys. Solids*, Vol. 3, No. 2, 1955. [https://doi.org/10.1016/0022-5096\(55\)90054-5](https://doi.org/10.1016/0022-5096(55)90054-5)
- [5] T.Z. Harmathy, Creep deflection of metal beams in transient heating processes, with particular reference to fire, *Can. J. Civ. Eng.*, Vol. 3, No. 2, pp. 219–228, 1976. <https://doi.org/10.1139/l76-022>
- [6] J.C. Chapman, B. Erickson, and N.J. Hoff, A theoretical and experimental investigation of creep buckling, *Int. J. Mech. Sci.*, Vol. 1, No. 2–3, pp. 145–174, 1960. [https://doi.org/10.1016/0020-7403\(60\)90037-0](https://doi.org/10.1016/0020-7403(60)90037-0)
- [7] J. Maljaars, J. Fellingner, and F. Soetens, Fire exposed aluminium structures, *Heron*, Vol. 50, No. 4, pp. 261–278, 2005.
- [8] J. Maljaars, F. Soetens, and H.H. Snijder, Local buckling of aluminium structures exposed to fire. Part 1: Tests, *Thin-Walled Struct.*, Vol. 47, No. 11, pp. 1404–1417, 2009. <https://doi.org/10.1016/j.tws.2009.02.008>

- [9] J. Maljaars, F. Soetens, and H.H. Snijder, Local buckling of aluminium structures exposed to fire. Part 2: Finite element models, *Thin-Walled Struct.*, Vol. 47, No. 11, pp. 1418–1428, 2009. <https://doi.org/10.1016/j.tws.2008.06.003>
- [10] E. Kandare, S. Feih, A. Kootsookos, Z. Mathys, B.Y. Lattimer, and A.P. Mouritz, Creep-based life prediction modelling of aluminium in fire, *Mater. Sci. Eng. A*, Vol. 527, No. 4–5, pp. 1185–1193, 2010. <https://doi.org/10.1016/j.msea.2009.10.010>
- [11] T.Z. Harmathy, A Comprehensive Creep Model, *J. Fluids Eng.*, Vol. 89, No. 3, pp. 496–502, 1967. <https://doi.org/10.1115/1.3609648>
- [12] H. Helman and G.J. Creus, A non-linear rheological model describing time-dependent deformations and failure, *Int. J. Non. Linear. Mech.*, Vol. 10, No. 3–4, pp. 167–172, 1975. [https://doi.org/10.1016/0020-7462\(75\)90034-7](https://doi.org/10.1016/0020-7462(75)90034-7)
- [13] N. Torić, I.U. Glavinić, and I.W. Burgess, Development of a rheological model for creep strain evolution in steel and aluminium at high temperature, *Fire and Materials*, Vol. 42, No. 8, pp. 879–888, 2018. <https://doi.org/10.1002/fam.2643>
- [14] N. Torić and I.W. Burgess, A unified rheological model for modelling steel behaviour in fire conditions, *J. Constr. Steel Res.*, Vol. 127, pp. 221–230, 2016. <https://doi.org/10.1016/j.jcsr.2016.07.031>
- [15] American Society for Testing and Materials (ASTM). ASTM E8/E8M-11, Standard Test Methods for Tension Testing of Metallic Materials, ASTM International: West Conshohocken, PA, USA, 2011.
- [16] American Society for Testing and Materials (ASTM). ASTM E21-09, Standard Test Methods for Elevated Temperature Tension Tests of Metallic Materials, ASTM International: West Conshohocken, PA, USA, 2009.
- [17] ANSYS, Inc. Canonsburg, PA 15317, Release 16.2, 2015.
- [18] M. Goreta, N. Torić, V. Divić, and I. Boko, Testing the influence of creep on fire-exposed aluminium columns, Proceedings of 9th International Congress of Croatian Society of Mechanics, pp. 1–10, September 2018.
- [19] N. Torić, I. Boko, I.W. Burgess and V. Divić, The effect of high-temperature creep on buckling behaviour of aluminium grade EN6082AW T6 columns, *Fire-Safety Journal*, Vol. 112, 2020. <https://doi.org/10.1016/j.firesaf.2020.102971>